ELSEVIER

Journal of Organometallic Chemistry 563 (1998) 137–146

Journal of Organometallic Chemistry

Organometallic complexes for nonlinear optics. 15. Molecular quadratic hyperpolarizabilities of *trans*-bis{bis(diphenylphosphino)methane}ruthenium σ-aryl- and σ-pyridyl-acetylides: X-ray crystal structure of *trans*-[Ru(2-C≡CC_5H_3N-5-NO_2)Cl(dppm)$_2$]

Raina H. Naulty [a], Andrew M. McDonagh [a], Ian R. Whittall [a], Marie P. Cifuentes [a], Mark G. Humphrey [a,*], Stephan Houbrechts [b], Joachim Maes [b], André Persoons [b], Graham A. Heath [c], David C.R. Hockless [c]

[a] *Department of Chemistry, Australian National University, Canberra, ACT 0200, Australia*
[b] *Centre for Research on Molecular Electronics and Photonics, Laboratory of Chemical and Biological Dynamics, University of Leuven, Celestijnenlaan 200D, B-3001 Leuven, Belgium*
[c] *Research School of Chemistry, Australian National University, Canberra, ACT 0200, Australia*

Received 29 January 1998; received in revised form 17 March 1998

Abstract

The complexes *trans*-[Ru(2-C≡CC_5H_3N-5-R)Cl(dppm)$_2$] [R = H (**6**), NO_2 (**7**)] have been prepared and **7** has been structurally characterized; comparison with the structural study of *trans*-[Ru(4-C≡C$C_6H_4NO_2$)Cl(dppm)$_2$] (**3**) reveals a decrease in Ru–C(1) distance and increase in Ru–Cl(1) distance, consistent with stronger σ-bonding by the nitropyridylalkynyl ligand in **7** compared to the nitrophenylalkynyl ligand in **3**. Electrochemical data for **3**, **6**, **7**, precursor dichloro complexes [$RuCl_2$(dppm)$_2$] [*cis* (**1a**), *trans* (**1b**)], and related alkynyl complexes *trans*-[Ru(4-C≡CC_6H_4R)Cl(dppm)$_2$] [R = H (**2**), 4-$C_6H_4NO_2$ (**4**), (*E*)-4-CH=C$HC_6H_4NO_2$ (**5**)] have been determined by cyclic voltammetry. Introduction of nitro substituent in progressing from **2** to **3** or **6** to **7** leads to a substantial increase in $E^o{}_{Ru}{}^{II/III}$, most of which is lost on chain-lengthening the alkynyl ligand in progressing from **3** to **4** or **5**. Replacement of phenyl by pyridyl in progressing from **2** to **6** or **3** to **7** results in a 0.1 V increase in $E^o{}_{Ru}{}^{II/III}$. The optical spectra of representative complexes have been examined. Introduction of a nitro substituent onto the phenylalkynyl ligand, in progressing from **2** to **3**, results in a substantial (ca. 11000 cm^{-1}) red-shift in the intense MLCT band of the Ru^{II}–C≡C–Ar–NO_2 moiety. Complexes **3**, **4** and **5** exhibit sizable solvatochromic shifts, suggestive of significant optical nonlinearities. Quadratic hyperpolarizabilities for **2**–**7** were determined by hyper-Rayleigh scattering (HRS) at 1064 nm; measurements are consistent with an increase in β_{HRS} upon incorporation of nitro substituent (progressing from **2** to **3** or **6** to **7**), chain-lengthening the alkynyl ligand (progressing from **3** to **4** and then to **5**) and replacing phenyl by pyridyl in progressing from **2** to **6**, general trends that are maintained with the two-level-corrected data, and which parallel shifts in λ_{max} to low energy. The observed and two-level-corrected β_{HRS} values for **7** are lower than expected; it is perhaps significant that λ_{max} for **7** is close to the second-harmonic.

Keywords: Acetylide; Alkynyl; Hyperpolarizability; Ruthenium; Nonlinear optics

1. Introduction

Organic molecules with a donor-bridge-acceptor composition have been shown to afford enhanced sec-

* Corresponding author. Tel.: +61 2 62492927; fax: +61 2 62490760; e-mail: Mark.Humphrey@anu.edu.au

0022-328X/98/$19.00
PII S0022-328X(98)00573-7

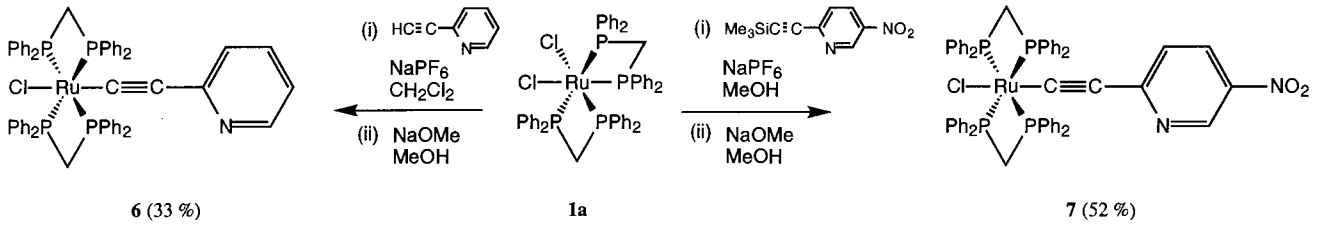

6 (33 %) **1a** **7** (52 %)

Scheme 1. Syntheses of pyridylacetylide complexes **6** and **7**.

ond-order nonlinear optical (NLO) responses [1–8]. With these precedents in mind, the optical nonlinearities of organometallic complexes have also come under scrutiny [8–13]. Organometallic complexes can be designed with a similar donor-bridge-acceptor composition, and have the additional flexibility of variable d electron count, oxidation state, and ligand environment, all of which may impact on NLO performance; they are therefore of significant interest. Our studies on complexes with this composition have focussed on metal σ-acetylides, compounds which have come under scrutiny for their third-order [14–17] as well as second-order NLO responses [18]. We have recently reported optical nonlinearities for 18 electron (cyclopentadienyl)bis(phosphine)ruthenium acetylides, 18 electron (cyclopentadienyl)(triphenylphosphine)nickel acetylides and 14 electron (triphenylphosphine)gold acetylides [19–23], in the process defining 'figures of merit' for the ligated metal centres as donor groups; the results of these studies revealed the NLO efficiency series [Ru] > [Ni] > [Au] for second-order responses by hyper-Rayleigh scattering β_{HRS}. It is also of interest to assess the importance of the co-ligands in the donor metal ligation sphere and, with this in mind, our attention has turned to an alternative ligated ruthenium system, namely *trans*-chlorobis(diphosphine)ruthenium acetylides. Complexes with this composition are also of interest as precursors to oligomers and/or polymers for third-order nonlinear optics [24]. This paper reports synthesis, spectroscopic (including solvatochromic), and electrochemical characterization of *trans*-chlorobis{bis(diphenylphosphino)methane}ruthenium acetylide complexes, their molecular quadratic optical nonlinearities at 1064 nm and their two-level-corrected values as determined by hyper-Rayleigh scattering (HRS), and comparison to computationally-derived nonlinearities at 1907 nm by ZINDO.

2. Results and discussion

2.1. Syntheses and characterization of σ-acetylide complexes

The synthetic methodology employed for the preparation of the new pyridyl acetylide complexes **6** and **7** is an extension of that successfully employed to synthesize analogous phenylacetylide complexes (Scheme 1) [25], the only significant difference being the utilization of the trimethylsilyl-protected acetylene rather than the terminal acetylene in the synthesis of the nitro complex **7**.

Complexes **6** and **7** were identified by IR-, ^{1}H-, ^{13}C-, and ^{31}P-NMR, and UV–vis spectroscopies, mass spectrometry, and satisfactory microanalyses. The infrared spectrum for **6** contains a characteristic ν(C≡C) band at 2080 cm^{-1}, similar to that of the analogous phenylacetylide **2** (2081 cm^{-1}). In contrast, the IR spectrum of the nitropyridylacetylide complex **7** contains a ν(C≡C) band at 2038 cm^{-1}, shifted substantially from that of the analogous nitrophenylacetylide complex **3** (2060 cm^{-1}) [25]. The ^{1}H-NMR spectra of **6** and **7** contain resonances assigned to phenyl and pyridyl hydrogens in the appropriate ratios, while the singlets at −5.7 (**6**) and −6.3 (**7**) ppm in the ^{31}P-NMR spectra confirm the *trans*-geometry of the bidentate phosphine ligands. In the UV–vis spectra, NO_2 substitution of the phenylacetylide is linked to a red-shift of 8000 cm^{-1} or more in the onset of strong absorption. Thus, the first intense band ($\varepsilon > 3000$ M^{-1} cm^{-1}) moves from ca. 32500 in **2** to ca. 21870 cm^{-1} in **3**, and moves from ca. 28500 in **6** to ca. 20500 in **7**. This long wavelength band in **3**, **7**, and their analogues, is assigned to the anticipated MLCT transition involving the readily oxidized Ru^{II} centre and the nitro-substituted arylacetylide (see later discussion). The mass spectra of **6** and **7** contain peaks corresponding to molecular ions, and fragment ions consistent with fragmentation proceeding via loss of the acetylide ligand followed by competitive loss of the chloride and one dppm ligand.

2.2. X-ray crystallographic study

A structural study of **7** was undertaken. Crystal data are given in Table 1 and selected bond lengths and angles are compiled in Table 2. Fig. 2 contains an ORTEP plot showing the molecular geometry and atomic labeling scheme.

A structural study of the nitrophenylacetylide analogue **3** has been completed previously [26], and a comparison of structural parameters with those from the current study are of obvious interest. The Ru–C(1)

Table 1
Crystallographic data for complex **7**

Empirical formula	$C_{57}H_{47}ClN_2O_{2.64}P_4Ru$
Molecular weight	1062.7
Crystal colour, Habit	Purple, plate
Crystal dimension (mm^3)	$0.16\times0.16\times0.04$
Space group	$P2_1/a$ (# 14)
Unit cell dimensions	
a (Å)	23.051(5)
b (Å)	10.199(6)
c (Å)	23.810(4)
β (°)	114.54(1)
V ($Å^3$)	5092(3)
Z	4
D_{calc} (g cm^{-3})	1.39
Trans. Factors	0.93–1.00
μ (cm^{-1})	(Cu–K_α) 45.26
N	8090
N_o [$I>3.00\sigma(I)$]	4736
No. variables	609
R	0.042
R_w	0.043

distance in **7** [1.949(6) Å] is significantly shorter than that in **3** [1.998(7) Å], but the C(1)–C(2) [1.201(8) Å (**7**), 1.190(8) Å (**3**)] and C(2)–C(3) [1.419(9) Å (**7**), 1.428(8) Å (**3**)] distances in these complexes are experimentally indistinguishable. Angles about the acetylide unit in **3** and **7** [Cl(1)–Ru(1)–C(1) 171.9(2)° (**7**), 177.7(2)° (**3**); Ru(1)–C(1)–C(2) 177.6(6)° (**7**), 176.8(5)° (**3**); C(1)–C(2)–C(3) 178.8(7)° (**7**), 168.4(7)° (**3**)] are close to linearity, with deviations presumably due to packing effects. The *trans* effect of the acetylide ligand, in this case manifested as differences in Ru–Cl(1) parameter, can possibly afford information about varying π*-back bonding in proceeding from phenylacetylide to pyridylacetylide. For the present pair of

Table 2
Important geometric parameters (Å, °) for complex 7

Ru(1)–C(1)	1.949(6)	C(6)–N(1)	1.450(8)
C(1)–C(2)	1.201(8)	N(1)–O(1)	1.227(8)
C(2)–C(3)	1.419(9)	N(1)–O(2)	1.247(8)
C(3)–C(4)	1.404(9)	Ru(1)–Cl(1)	2.512(2)
C(4)–C(5)	1.358(9)	Ru(1)–P(1)	2.350(2)
C(5)–C(6)	1.37(1)	Ru(1)–P(2)	2.370(2)
C(6)–C(7)	1.373(9)	Ru(1)–P(3)	2.339(2)
C(7)–N(8)	1.326(8)	Ru(1)–P(4)	2.337(2)
N(8)–C(3)	1.362(8)		
Cl(1)–Ru(1)–C(1)	171.9(2)	C(6)–C(7)–N(8)	123.6(7)
Ru(1)–C(1)–C(2)	177.6(6)	C(7)–N(8)–C(3)	116.5(7)
C(1)–C(2)–C(3)	178.8(7)	C(6)–N(1)–O(1)	119.1(7)
C(2)–C(3)–N(8)	116.9(6)	C(6)–N(1)–O(2)	118.6(7)
C(2)–C(3)–C(4)	121.3(7)	O(1)–N(1)–O(2)	122.3(7)
N(8)–C(3)–C(4)	121.8(6)	P(1)–Ru(1)–P(2)	70.61(6)
C(3)–C(4)–C(5)	120.3(7)	P(3)–Ru(1)–P(4)	70.90(6)
C(4)–C(5)–C(6)	117.3(7)	P(1)–Ru(1)–P(3)	107.28(6)
C(5)–C(6)–C(7)	120.5(7)	P(2)–Ru(1)–P(4)	110.46(6)

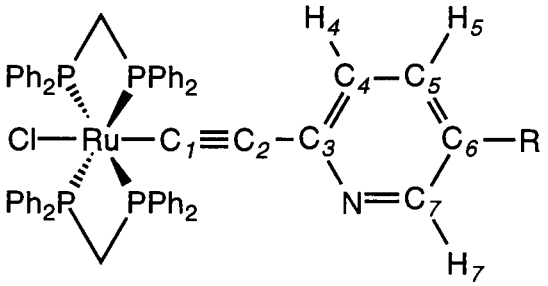

Fig. 1. Numbering scheme for NMR spectral assignments of **6** (R = H_6) and **7** (R = NO_2).

complexes, replacement of phenyl by pyridyl in proceeding from **3** to **7** results in an increase in Ru–Cl(1) distance from 2.483(2) Å (**3**) to 2.512(2) Å (**7**), consistent with an increase in *trans* influence upon introduction of pyridyl group. It is usually difficult to deconvolute the σ and π contributions to bonding; in the present case, incorporation of pyridyl may increase π-acceptance by the acetylide ligand, or alternatively, increase σ-donation by the acetylide group, both of which will result in a stronger and shorter M–C bond. Because the chloride ligand is a σ-donor and π-donor, increased σ-donation by the acetylide ligand should weaken the Ru–Cl(1) linkage, and increased π-acceptance by the acetylide should strengthen the Ru–Cl(1) bond. As Ru–Cl(1) is weakened in proceeding from **3** to **7**, it seems likely that replacement of phenyl by pyridyl bridge in the alkynyl group serves to enhance σ-bonding rather than π-acceptance. The Ru-P distances [2.337(2)–2.370(2) Å (**7**), 2.332(2)–2.379(2) Å (**3**)] are similar. Distances within the nitropyridyl group and intraphosphine bond lengths and angles are not unusual.

2.3. Electrochemical studies

The quadratic optical nonlinearities of donor-bridge-acceptor organic compounds are correlated to the strength of the appended donor and acceptor substituents. It is therefore of interest to assess the donor and/or acceptor strength of the corresponding components in organometallic complexes and relate these to the NLO response. We have previously examined 18-electron cyclopentadienyl-ruthenium and -nickel nitrophenylacetylide complexes electrochemically [27]. The $M^{II/III}$ couple occurs at lower potential for ruthenium; correspondingly, the ruthenium complexes have higher quadratic optical nonlinearities than their nickel analogues. We have now extended these studies in the present work to embrace the 18 electron chloro-bis{bis(diphenylphosphino)methane}ruthenium acetylide complexes, the results being presented in Table 3.

Table 3
Cyclic voltammetric data for complexes **1**–**7**[a]

Complex	E°_{Ru} (V)	i_{pc}/i_{pa}	$E^{\circ}_{NO_2}$ (V)	i_{pa}/i_{pc}
cis-[$RuCl_2(dppm)_2$] (**1a**)	1.00	1.0	–	–
trans-[$RuCl_2(dppm)_2$] (**1b**)	0.62	1.0	–	–
trans-[$Ru(C{\equiv}CPh)Cl(dppm)_2$] (**2**)	0.55	1.0	–	–
trans-[$Ru(4\text{-}C{\equiv}CC_6H_4NO_2)Cl(dppm)_2$] (**3**)	0.72	0.9	−1.08	0.7
trans-[$Ru(4,4'\text{-}C{\equiv}CC_6H_4C_6H_4NO_2)Cl(dppm)_2$] (**4**)	0.58	0.9	−0.94	0.5
trans-[$Ru((E)\text{-}4,4'\text{-}C{\equiv}CC_6H_4CH{=}CHC_6H_4NO_2)Cl(dppm)_2$] (**5**)	0.56	1.0	−0.87	0.4
trans-[$Ru(2\text{-}C{\equiv}CC_5H_4N)Cl(dppm)_2$] (**6**)	0.66	0.9	–	–
trans-[$Ru(2\text{-}C{\equiv}CC_5H_3N\text{-}5\text{-}NO_2)Cl(dppm)_2$] (**7**)	0.81	0.9	−0.95	1.0

[a] At −50°C vs. Ag/AgCl; 0.5 M [NBu^n_4][PF_6] in CH_2Cl_2 with a rate of 100 mV s^{-1}, using the ferrocene/ferrocenium couple as an internal standard.

Oxidation potentials for the precursor chloro complexes are found at 1.00 V (**1a**) and 0.62 V (**1b**). As expected, oxidation is easier for the *trans*-compound where the redox-active (doubly-degenerate) d_{xz}, d_{yz} orbitals interact with two mutually *trans* Cl^- ligands and two mutually *trans* P-donors. Replacing chloride by phenylacetylide in proceeding from **1b** to **2** results in a small decrease (0.07 V) in $E^{\circ}_{Ru^{II/III}}$, indicating that phenylacetylide marginally exceeds Cl^- in ability to favour oxidation. Appending a nitro substituent to the phenylacetylide (progressing from **2** to **3**) leads as expected to a sizable increase in oxidation potential (0.17 V); essentially the same effect (0.15 V) appears for **6** vs. **7**, and a similar increase (0.18 V) was seen in the cyclopentadienylruthenium system [27]. Chain-lengthening of the acetylide ligand (one-ring to two-ring) leads to a decrease in $E^{\circ}_{Ru^{II/III}}$, to the extent that the metals in **4** and **5** are not much more difficult to oxidize than the metal in the non-nitro complex, **2**; again, a similar effect was observed in the cyclopentadienylruthenium system [22]. The greatest interest in the current work lies in comparison between analogous phenyl- and pyridyl-acetylide complexes. Proceeding from **2** to **6** and from **3** to **7** results in increases of 0.11 and 0.09 V, respectively. The nitro-based reduction couple is observed at −1.08 (**3**) and −0.95 V (**7**). The effect of pyridyl incorporation (c.f. phenylene linkage) is thus to favour reduction and disfavour oxidation. The former effect possibly results from charge localization at the electronegative nitrogen; charge density calculations may shed light on this. For the donor-acceptor cyclopentadienyl-ruthenium and -nickel acetylide complexes we examined previously, the parameter $E^{\circ}_{M^{II/III}} - E^{\circ}_{NO_2/NO_2^-}$ was correlated with quadratic hyperpolarizability (though cautiously, given departures from reversibility) [27]. The values of this parameter for **3** (1.80 V) and **7** (1.76 V) suggest a small increase in nonlinearity in proceeding from **3** to **7**, and accord with the slight red-shift of the MLCT band, which is achieved despite $E^{\circ}_{Ru^{II/III}}$ being more difficult for **7** (although differences are minor). Comparison of this parameter for **3** (1.80 V), **4** (1.52 V) and **5** (1.43 V) with those of the analogous cyclopentadienylruthenium complexes [$Ru(4\text{-}C{\equiv}CC_6H_4NO_2)(PPh_3)_2(\eta\text{-}C_5H_5)$] (1.81 V), [$Ru(4,4'\text{-}C{\equiv}CC_6H_4C_6H_4NO_2)(PPh_3)_2(\eta\text{-}C_5H_5)$] (1.50 V) and [$Ru((E)\text{-}4,4'\text{-}C{\equiv}CC_6H_4CH{=}CHC_6H_4NO_2)(PPh_3)_2(\eta\text{-}C_5H_5)$] (1.47 V), respectively, suggests that nonlinearities should vary little upon replacing the (cyclopentadienyl)bis(triphenylphosphine)ruthenium donor by the chlorobis{bis(diphenylphosphino)methane}ruthenium donor, if these data have predictive merit.

2.4. Solvatochromic behaviour

Given the relative ease of oxidation and reduction of the archetypal Ru^{II} nitrophenylacetylide complex **3**, with an electrode potential gap of only 1.8 V, it is not surprising to find that it is highly coloured (deep purple) with a distinctive intense optical band maximum in the near-UV region. The optical spectra of three instructive species (**1b**, **2** and **3**) in diethyl ether solution are displayed in Fig. 3. Comparison of **3** with the parent *trans*-dichloride (**1b**) shows very clearly how the planar $Ru^{II}P_4$ chromophore is responsible for the three features observed above 30000 cm^{-1}, whereas the new feature in **3**, at 21870 cm^{-1}, is due to the Ru^{II}-C≡C–Ar–NO_2 moiety. The weak band at 31020 cm^{-1} and the intense bands at 36670 and 37370 cm^{-1} are collectively ascribed to charge-transfer within the $Ru^{II}P_4$ moiety, by analogy with previous studies on *trans*-[$RuCl_2(PR_3)_4$] and related systems [28,29]. The multiplet structure of the first intense band (near 36700 cm^{-1}) is very characteristic of the presence of the phenyl substituents on the phosphine, but similarly located CT bands (without the structure) are also present for trialkylphosphine Ru^{II} derivatives such as *trans*-[$RuCl_2(PMe_3)_4$]. Replacing Cl^- by phenylacetylide, in proceeding from **1b** to **2**, significantly increases the lowest frequency absorption. It is probable that the band at 32500 cm^{-1} is a superposition of weak bands corresponding to the $Ru^{II}P_4$ chromophore and an intense CT band involving the phenylacetylide ligand.

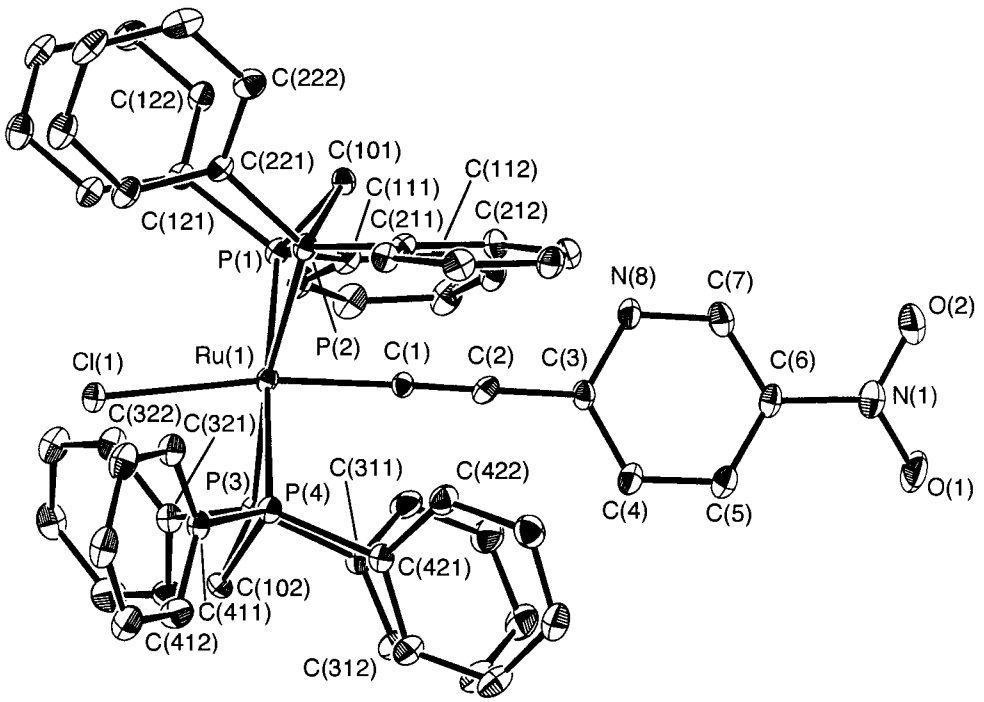

Fig. 2. Molecular geometry and atomic labeling scheme for *trans*-[Ru(2-C≡CC$_5$H$_3$N-5-NO$_2$)Cl(dppm)$_2$] (**7**). 20% thermal ellipsoids are shown for the non-hydrogen atoms; hydrogen atoms are omitted for clarity.

Accordingly, introduction of the NO_2 substituent, in proceeding from **2** to **3**, can be regarded as red-shifting the crucial CT band by 11000 cm^{-1} from 32500 to 21870 cm^{-1}. A commensurate red-shift (8000 cm^{-1}) can be found when **6** is compared with **7**.

Sizable solvent-induced shifts in absorption maxima (solvatochromism) have been taken to indicate complexes with appreciable quadratic molecular hyperpolarizabilities β [30]. Solvatochromic behaviour has even been used (in combination with other measurable parameters) to calculate the nonlinearities of some dimesitylboron-containing complexes [31]. It was therefore of interest to assess the solvatochromic response of the MLCT band for some representative examples of chloro{bis(bis(diphenylphosphino)methane}ruthenium acetylide complexes. Data for **3**, **4** and **5** across a range of solvents are collected in Table 4.

Complexes **3**, **4** and **5** have solvatochromic shifts of 1410 cm^{-1} (31 nm), 860 cm^{-1} (18 nm) and 730 cm^{-1} (17 nm), respectively, across the range of solvents employed, with the lowest energy transition found in the polar solvent dmf in each case. These sizable solvatochromic shifts suggest that donor-bridge-acceptor organometallic acetylides may have significant quadratic nonlinearities. With this in mind, the NLO merit of complexes **2**–**7** was assessed.

2.5. Quadratic hyperpolarizabilities

Experimentally obtained data for **2**–**7** at 1064 nm by hyper-Rayleigh scattering and two-level-corrected values are collected in Table 5, together with the previously-reported computationally-derived data at 1907 nm by ZINDO for **2**–**5**. Experimentally-obtained and two-level-corrected quadratic NLO data confirm trends previously noted with other metal acetylide complexes [20–23]. The β values increase upon incorporation of the nitro substituent (progressing from **2** to **3** or **6** to **7**) and chain-lengthening the alkynyl ligand (progressing from **3** to **4** to **5**). The previously reported ZINDO derived data [25] are consistent with these trends, but absolute values differ significantly. ZINDO has been used with success in computing quadratic nonlinearities of ferrocenyl complexes, the results from which reproduce experimental data [32,33]. However, the wavelength for computation (1907 nm) differs from that of experiment (1064 nm) in the present case. Additionally, it should be noted that ZINDO computes gas phase data rather than solution nonlinearities. Taken together, these factors are consistent with ZINDO reproducing relative NLO merit rather than absolute values. The effect of replacing phenylalkynyl by pyridylalkynyl ligand is unclear; β values increase on proceeding from **2** to **6**, but decrease on proceeding from **3** to **7**. Introduction of the heterocyclic ring with diminished aromatic stabilization energy is expected to lead to an increase in nonlinearity [34–36]; the lower-than-expected experimental and two-level-corrected β values for **7** may possibly be due to the proximity of λ_{max} to the second-harmonic frequency. The observed and two-

Table 4
Solvatochromic behaviour of complexes **3**–**5**

Complex	ν_{min} (cm^{-1})[a]			
	Cyclohexane (2.0)	Diethyl ether (4.3)	Acetone (20.7)	Dimethylformamide (36.7)
trans-[Ru(4-C≡$CC_6H_4NO_2$)Cl(dppm)$_2$] (**3**)	22 130	21 870	21 140	20 720
trans-[Ru(4,4′-C≡$CC_6H_4C_6H_4NO_2$)Cl(dppm)$_2$] (**4**)	22 100	22 080	21 900	21 480
trans-[Ru((*E*)-4,4′-C≡CC_6H_4CH=$CHC_6H_4NO_2$)Cl(dppm)$_2$] (**5**)	20 510	20 830	20 810	20 490

[a] Optical transition frequency data ordered by solvent (dielectric constant).

level-corrected data for **5** are amongst the largest thus far for organometallic complexes.

If the lowest energy (MLCT) transitions are contributing significantly to the observed nonlinearities, then a nonlinearity-transparency trade-off should be observed. Fig. 4 contains a logarithmic plot exploring this possibility by correlating β and λ_{max}. Experimentally-determined data are dispersively enhanced, but correlation with two-level-corrected values is not significantly better. The correlation for the present class of complexes is certainly poorer than that observed with donor-acceptor substituted stilbenes [37], emphasizing that the two-state model may not be appropriate for organometallic complexes.

Fig. 5 correlates quadratic optical nonlinearities for the *trans*-bis{bis(diphenylphosphino)methane}ruthenium acetylide complexes **3**–**5** with those of precursor terminal alkynes, and includes data for the previously reported (cyclopentadienyl)bis(triphenylphosphine) ruthenium [22], (cyclopentadienyl)(triphenylphosphine)nickel [23], and (triphenylphosphine)gold [21] acetylide systems. The slopes of the graphs for the new complexes (29.6 ($R = 1.00$) for experimental data; 5.2 ($R = 0.95$) for two-level corrected values) are comparable to those of the previously reported ruthenium acetylide series (24.2 ($R = 0.98$) for experimental data; 6.7 ($R = 0.69$) for two-level corrected values), and significantly larger than those for the related nickel (6.4 (0.93); 3.6 (0.94)) and gold (2.4 (0.99); 2.0 (0.99)) acetylides. [Note: the coefficient for the two-level-corrected data for the cyclopentadienylruthenium acetylide series ($R = 0.69$) is consistent with no correlation, probably a result of the lack of applicability of the two-level model for these complexes]. We have previously utilized this data to define tentative 'figures of merit' to quantify the efficiency of the ligated metal centres as donors in these donor-bridge-acceptor complexes. The results herein suggest that the nature of the metal (Ru versus Ni or Au) is more important than variations in the ligand environment [Cl(dppm)$_2$ versus (PPh_3)$_2$(η-C_5H_5)] for the present series of complexes.

3. Experimental

3.1. General

All organometallic reactions were carried out under an atmosphere of nitrogen with the use of standard Schlenk techniques; no attempt was made to exclude air during work-up of products. Dichloromethane was distilled over CaH_2. Petroleum ether refers to a fraction of boiling range 60–80°C. $NaPF_6$ (Aldrich) was recrystallized from hot acetonitrile. 2-HC≡CC_5H_4N [38], 2-Me_3SiC≡CC_5H_3N-5-NO_2 [27], *cis*-[$RuCl_2$(dppm)$_2$] (**1a**) [39], *trans*-[$RuCl_2$(dppm)$_2$] (**1b**), [40] *trans*-[Ru(C≡CPh)Cl(dppm)$_2$] (**2**), *trans*-[Ru(4-C≡$CC_6H_4NO_2$)Cl-(dppm)$_2$] (**3**), *trans*-[Ru(4,4′-C≡$CC_6H_4C_6H_4NO_2$)Cl-(dppm)$_2$] (**4**), and *trans*-[Ru((*E*)-4,4′-C≡CC_6H_4CH = $CHC_6H_4NO_2$)Cl(dppm)$_2$] (**5**) [25] were prepared following the literature methods. Column chromatography was carried out using Merck 7734 Kieselgel 60 silica for purification of organic products and Merck aluminium oxide 90 active basic (activity stage III, 70–230 mesh ASTM) for purification of organometallic complexes. Microanalyses were performed at the Research School of Chemistry, Australian National University. Infrared spectra were recorded using a Perkin-Elmer System 2000 FT-IR spectrometer. UV–vis spectra were recorded using a Cary 5 spectrophotometer. Electrochemical measurements were carried out using a Princeton Applied Research Model 170 Potentiostat. The supporting electrolyte was [NBu^n_4][PF_6] (0.5 M) in distilled deoxygenated CH_2Cl_2. Solutions (1×10^{-3} M) were made under a purge of nitrogen and measured versus a Ag/AgCl reference electrode at −50°C, such that the ferrocene/ferrocenium redox couple was located at 0.55 V. ^{1}H-, ^{13}C- and ^{31}P-NMR spectra were recorded using a Varian Gemini-300 FT NMR spectrometer and are referenced to residual $CHCl_3$, 7.24 ppm, $CDCl_3$, 77.0 ppm, and external 85% H_3PO_4, 0.0 ppm, respectively. NMR spectral assignments for **6** and **7** follow the numbering scheme shown in Fig. 1.

Table 5
Experimental linear optical spectroscopic and quadratic nonlinear optical response parameters[a]

Compound	λ (nm) (ε (10^4 M^{-1} cm^{-1}))	β_{1064} (10^{-30} esu)[b]	$\beta_{1064,\ corr}$ (10^{-30} esu)[c]	$\beta_{vec,1907}$ (10^{-30} esu)[d]
trans-[Ru(C≡CPh)Cl(dppm)$_2$] (**2**)	308 (1.7)	20	12	−13
trans-[Ru(4-C≡CC$_6$H$_4$NO$_2$)Cl(dppm)$_2$] (**3**)	473 (1.8), 312 (0.6) sh	767	129	34
trans-[Ru(4,4′-C≡CC$_6$H$_4$C$_6$H$_4$NO$_2$)Cl(dppm)$_2$] (**4**)	465 (1.7), 320 (2.0)	933	178	45
trans-[Ru((*E*)-4,4′-C≡CC$_6$H$_4$CH=CHC$_6$H$_4$NO$_2$)Cl(dppm)$_2$] (**5**)	490 (2.6), 349 (2.4)	1964	235	60
trans-[Ru(2-C≡CC$_5$H$_4$N)Cl(dppm)$_2$] (**6**)	351 (1.2)	35	19	
trans-[Ru(2-C≡CC$_5$H$_3$N-5-NO$_2$)Cl(dppm)$_2$] (**7**)	490 (1.8), 326 (0.7)	468	56	

[a] All measurements in thf solvent. All complexes are optically transparent at 1064 nm.
[b] HRS at 1064 nm; values ± 10%.
[c] HRS at 1064 nm corrected for resonance enhancement at 532 nm using the two-level model with $\beta_o = \beta[1-(2\lambda_{max}/1064)^2][1-(\lambda_{max}/1064)^2]$; damping factors not included.
[d] ZINDO-derived data at 1907 nm. Ref. [25].

3.2. Syntheses

3.2.1. Trans-[Ru(C≡C-2-C$_5$H$_4$N)Cl(dppm)$_2$] (6)

Cis-[RuCl$_2$(dppm)$_2$] (200 mg, 0.21 mmol), $NaPF_6$ (100 mg, 0.61 mmol) and 2-pyridylacetylene (50 mg, 0.48 mmol) were added to dichloromethane (10 ml), and stirred for 4 h at r.t.. NaOMe (1 M in methanol, 4 ml) and petroleum ether (10 ml) were added and the mixture passed through an alumina plug. The solvents were removed under reduced pressure and the resulting residue purified by column chromatography using 50/50 dichloromethane/petroleum ether as eluant, yielding 75 mg (33%) of the yellow product. Anal. Calcd for $C_{57}H_{48}ClNP_4Ru \cdot CH_2Cl_2$: C 63.77, H 4.62, N 1.28%. Found: C 64.11, H 4.38, N 1.35%. IR: (CH_2Cl_2) ν(C≡C) 2080 cm^{-1}. UV–vis: λ (thf) 351 nm, ε 11800 M^{-1} cm^{-1}. ^{1}H-NMR: (δ, 300 MHz, $CDCl_3$); 4.82 (m, 2H, CH_2), 5.16 (m, 2H, CH_2), 5.28 (s, 2H, CH_2Cl_2), 5.42 (d, $J_{HH} = 8$ Hz, 1H, H_4), 6.68 (m, 1H, H_5), 6.97–7.54 (m, 40H, Ph), 8.22 (m, 1H, H_7). Resonance for H_6 is obscured by the resonances of the phenyl hydrogens. ^{13}C-NMR: (δ, 75 MHz, $CDCl_3$); 117.0 (C_2), 127.5 (C_p), 128.4 (C_5), 129.1 (d, $J_{CP} = 30$ Hz, C_m), 133.4 (d, $J_{CP} = 39$ Hz, C_o), 134.4 (m, C_i). C_1, C_3, C_4, C_6 and C_7 were not detected. ^{31}P-NMR: (δ, 121 MHz, $CDCl_3$); −5.7. FAB MS; m/z (fragment, relative intensity): 1007 ($[M]^+$, 50), 869 ($[Ru(dppm)_2\text{-}H]^+$, 44), 588 ([M-(dppm)-Cl]$^+$, 21), 486 ($[Ru(dppm)]^+$, 50).

3.2.2. Trans-[Ru(C≡C-2-C$_5$H$_3$N-5-NO$_2$)Cl(dppm)$_2$] (7)

Cis-[RuCl$_2$(dppm)$_2$] (50 mg, 0.05 mmol), $Me_3SiC{\equiv}C$-2-C_5H_3N-5-NO_2 (9 mg, 0.04 mmol) and $NaPF_6$ (9 mg, 0.05 mmol) were added to methanol (10 ml). Sodium (2 mg, 0.09 mmol) was then added, and the reaction mixture allowed to stir for 20 h. The solvent was removed in vacuo and the residue extracted into dichloromethane. The product was then adsorbed onto alumina and subjected to column chromatography with 50/50 dichloromethane/petroleum ether as eluant. The first, purple band was eluted and the dichloromethane removed on a rotary evaporator. Filtration yielded 22 mg (52%) of the deep purple product. Anal. Calcd for $C_{57}H_{47}N_2ClO_2P_4Ru$: C 65.04, H 4.50, N 2.66%. Found: C 64.33, H 4.46, N 2.41%. IR: (CH_2Cl_2) ν(C≡C) 2038 cm^{-1}. UV–vis: λ (thf) 490 nm, ε 18900 M^{-1} cm^{-1}. ^{1}H-NMR: (δ, 300 MHz, $CDCl_3$); 4.84 (m, 2H, CH_2), 5.10 (m, 2H, CH_2), 5.22 (d, $J_{HH} = 9$ Hz, 1H, H_4), 7.03–7.50 (m, 40H, Ph), 7.72 (dd, $J_{HH} = 9$ Hz, $J_{HH} = 3$ Hz, 1H, H_5), 9.10 (d, $J_{HH} = 3$ Hz, 1H, H_7). ^{13}C-NMR: (δ, 75 MHz, $CDCl_3$); 48.3 (CH_2), 119.8 (C_2), 124.8 (C_4), 127.7 (C_p), 128.6 (C_5), 129.4 (d, $J_{CP} = 29$ Hz, C_m), 133.3 (d, $J_{CP} = 50$ Hz, C_o), 134.2 (m, C_i), 138.1 (C_3), 145.4 (C_7), 150.9 (C_6). C_1 was not observed. ^{31}P-NMR: (δ, 121 MHz, $CDCl_3$); −6.3. FAB MS; m/z (fragment, relative intensity): 1052 ($[M]^+$, 100), 869 ($[Ru(dppm)_2\text{-}H]^+$, 32), 633 ([M-(dppm)-Cl]$^+$, 33), 485 ($[Ru(dppm)\text{-}H]^+$, 24). A crystal suitable for X-ray diffraction analysis was grown by diffusion of hexane into a dichloromethane solution at −5°C.

3.3. Crystallography

A unique diffractometer data set was obtained on a Rigaku AFC6R diffractometer using the $\omega - 2\theta$ scan technique (graphite monochromated Cu–K_α radiation; 1.54178 Å; $2\theta_{max} = 120°$; 193 K) and yielded N independent reflections, N_o of these with $I \geq 3.00\sigma(I)$ being considered 'observed' and used in full matrix least squares refinement; an empirical psi-type absorption correction was applied. Anisotropic thermal parameters were refined for all non-hydrogen atoms except the oxygen of a disordered solvent molecule which refined to partial occupancy; (x, y, z, $U_{iso})_H$ were included constrained at estimated values. Conventional residuals R and R_w on $|F|$ are given; the weighting function $w = 1/\sigma^2(F_o^2) = [\sigma_c^2(F_o) + (p^2/4)F_o^2]^{-1}$ [$\sigma_c^2(F_o)$ = estimated S.D. based on counting statistics, $p = p$ factor determined experimentally from standard reflections]

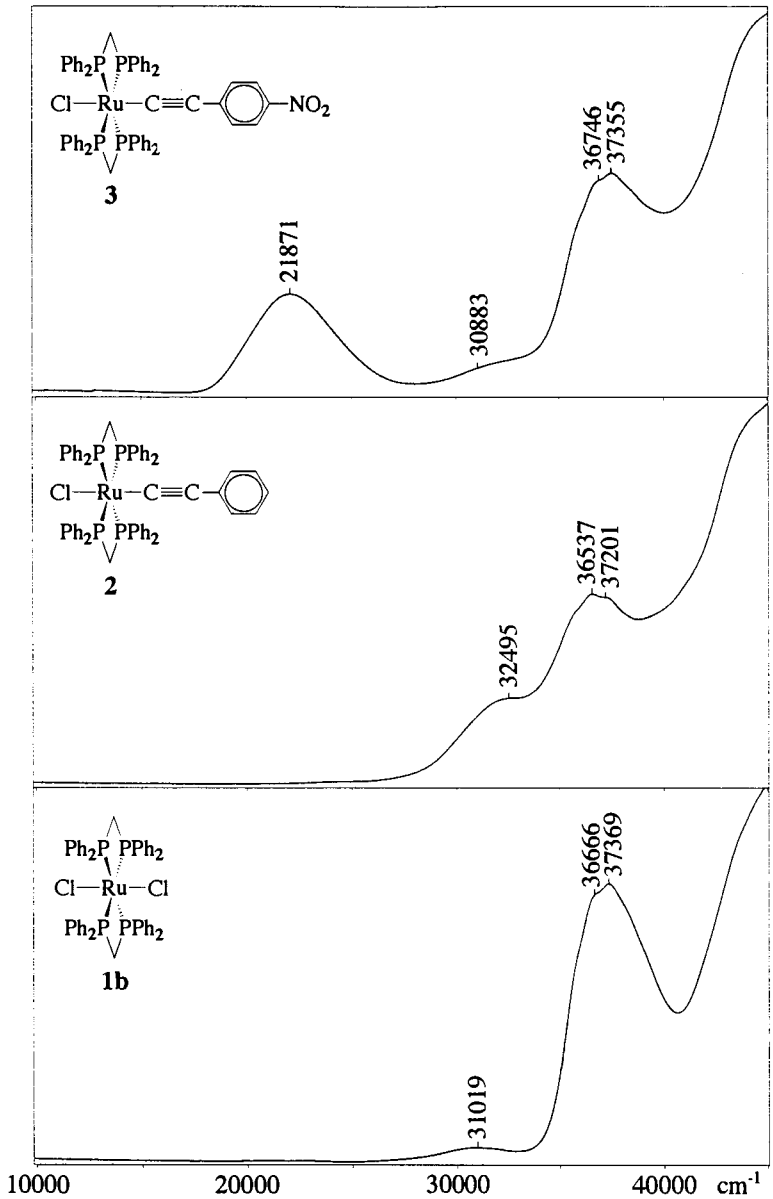

Fig. 3. Optical spectra for **1b**, **2**, and **3**.

was employed. Computation used the teXsan package [41]. Specific data collection, solution and refinement parameters are given in Table 1. Pertinent results are given in the figure and tables.

3.4. HRS Measurements

An injection-seeded Nd:YAG laser (Q-switched Nd:YAG Quanta Ray GCR5, 1064 nm, 8 ns pulses, 10 Hz) was focussed into a cylindrical cell (7 ml) containing the sample. The intensity of the incident beam was varied by rotation of a half-wave plate placed between crossed polarizers. Part of the laser pulse was sampled by a photodiode to measure the vertically polarized incident light intensity. The frequency doubled light was collected by an efficient condenser system and detected by a photomultiplier. The harmonic scattering and linear scattering were distinguished by appropriate filters; gated integrators were used to obtain intensities of the incident and harmonic scattered light. All measurements were performed in thf using p-nitroaniline ($\beta = 21.4 \times 10^{-30}$ esu [42]) as a reference. Further details of the experimental procedure have been reported elsewhere [43–45].

4. Conclusion

The donor-bridge-acceptor composition for organometallic σ-acetylide complexes in the present

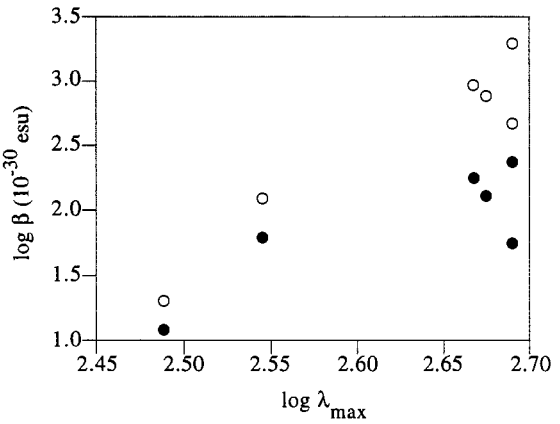

Fig. 4. Logarithmic plot of β versus λ_{max} for complexes **2**–**7**; (○) experimental data, (●) two-level-corrected values.

work has afforded molecules with the largest quadratic optical nonlinearities for organometallic systems thus far observed. Our earlier studies emphasized the importance of metal valence electron count and ease of oxidation at the metal centre for quadratic NLO merit. The present studies have complemented the earlier reports by extending work with the most effective metal (ruthenium) to a different ligation environment. Results indicate that replacing $(PPh_3)_2(\eta\text{-}C_5H_5)$ by $Cl(dppm)_2$ does not impact significantly on quadratic optical nonlinearity. It is possible that more dramatic co-ligand variation (e.g. replacing soft donor P-ligands by hard donor N-ligands, or by electron withdrawing CO ligands) may affect quadratic NLO merit rather more substantially; these variations will be the subject of future reports. Chromophore modification for the present series of complexes (introduction of nitro substituent, acetylide poly-aryl chain-lengthening, bridge modification, replacement of phenyl by pyridyl) has in almost all instances resulted in increases in nonlinearity, as expected from results with organic molecules. In the present work, we have conclusively identified the intense low energy band in the electronic spectra of the donor-bridge-acceptor σ-acetylide complexes as being MLCT to the acetylide ligand in origin. Correlation of β values with λ_{max} of this MLCT transition is inferior, consistent with a lack of applicability of the two-level model.

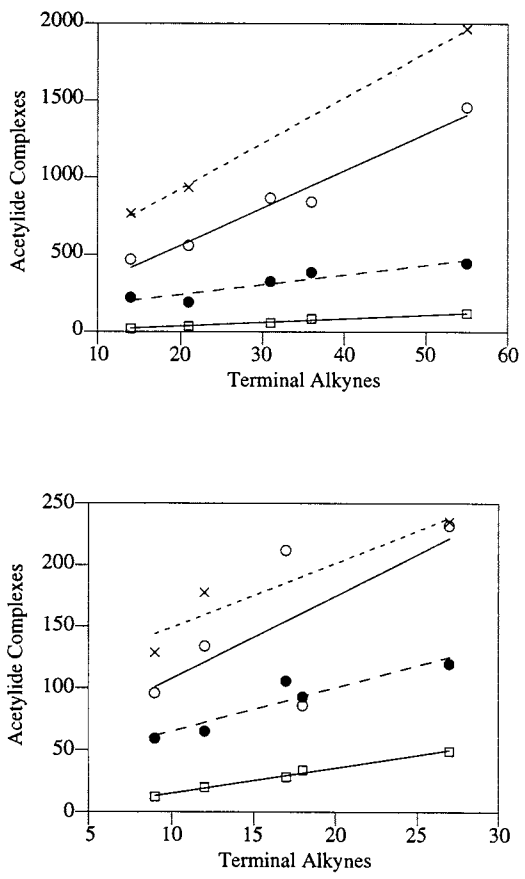

Fig. 5. Correlation of molecular quadratic hyperpolarizabilities of complexes **3**–**5** (x) and related metal acetylide complexes [(cyclopentadienyl)bis(triphenylphosphine)ruthenium acetylides (○),[17] (cyclopentadienyl)(triphenylphosphine)nickel acetylides (●),[18] (triphenylphosphine)gold acetylides (□)[16]] with those of the corresponding terminal alkynes (10^{-30} esu) (a) experimental data; (b) two-level corrected values. 10% uncertainty.

Acknowledgements

We thank the Australian Research Council (MGH), the Institute of Advanced Studies (GAH), the Belgian Government (Grant No. IUAP-P4-11) (AP), the Fund for Scientific Research-Flanders (Grant No. G.0308.96) (AP), and the University of Leuven (Grant No. GOA 95/1) (AP) for support of this work, and Johnson–Matthey Technology Centre (MGH) for the loan of ruthenium salts. A.M.M. is the recipient of an Australian Postgraduate Award, M.P.C. holds an ARC Australian Postdoctoral Research Fellowship, M.G.H. holds an ARC Australian Research Fellowship, and S.H. is a Research Assistant of the Fund for Scientific Research-Flanders.

References

[1] R.A. Hann, D. Bloor (Eds.), Organic Materials for Non-linear Optics, Royal Society of Chemistry, London, 1989.
[2] R.A. Hann, D. Bloor (Eds.), Organic Materials for Non-linear Optics II, Royal Society of Chemistry, London, 1991.
[3] G.J. Ashwell, D. Bloor (Eds.), Organic Materials for Non-linear Optics III, Royal Society of Chemistry, Cambridge, 1993.
[4] S.R. Marder, J.E. Sohn, G.D. Stucky (Eds.), Materials for Nonlinear Optics, Chemical Perspectives, American Chemical Society, Washington DC, 1991.
[5] D.S. Chemla, J. Zyss (Eds.), Nonlinear Optical Properties of Organic Molecules and Crystals I, Academic Press, Orlando, 1987.

[6] D.S. Chemla, J. Zyss (Eds.), Nonlinear Optical Properties of Organic Molecules and Crystals II, Academic Press, Orlando, 1987.
[7] J. Messier, F. Kajzar, P. Prasad (Eds.), Organic Molecules for Nonlinear Optics and Photonics, Kluwer, Dordrecht, 1991.
[8] T. Verbiest, S. Houbrechts, M. Kauranen, K. Clays, A. Persoons, J. Mater. Chem. 7 (1997) 2175.
[9] I.R. Whittall, A.M. McDonagh, M.G. Humphrey, M. Samoc, Adv. Organomet. Chem. 42 (1998) 291.
[10] I.R. Whittall, A.M. McDonagh, M.G. Humphrey, M. Samoc, Adv. Organomet. Chem. 43 (1998) 349.
[11] S.R. Marder, in: D.W. Bruce, D. O'Hare (Eds.), Inorganic Materials, Wiley, Chichester, 1992, p. 116.
[12] N.J. Long, Angew. Chem, Int. Ed. Engl. 34 (1995) 21.
[13] H.S. Nalwa, Appl. Organomet. Chem. 5 (1991) 349.
[14] L.K. Myers, C. Langhoff, M.E. Thompson, J. Am. Chem. Soc. 114 (1992) 7560.
[15] L.K. Myers, D.M. Ho, M.E. Thompson, C. Langhoff, Polyhedron 14 (1995) 57.
[16] P.L. Porter, S. Guha, K. Kang, C.C. Frazier, Polymer 32 (1991) 1756.
[17] C.C. Frazier, S. Guha, W.P. Chen, M.P. Cockerham, P.L. Porter, E.A. Chauchard, C.H. Lee, Polymer 28 (1987) 553.
[18] P. Nguyen, G. Lesley, T.B. Marder, I. Ledoux, J. Zyss, Chem. Mater. 9 (1997) 406.
[19] I.R. Whittall, M.G. Humphrey, D.C.R. Hockless, B.W. Skelton, A.H. White, Organometallics 14 (1995) 3970.
[20] I.R. Whittall, M.G. Humphrey, A. Persoons, S. Houbrechts, Organometallics 15 (1996) 1935.
[21] I.R. Whittall, M.G. Humphrey, S. Houbrechts, A. Persoons, D.C.R. Hockless, Organometallics 15 (1996) 5738.
[22] I.R. Whittall, M.P. Cifuentes, M.G. Humphrey, B. Luther-Davies, M. Samoc, S. Houbrechts, A. Persoons, G.A. Heath, D.C.R. Hockless, J. Organomet. Chem. 540 (1997) 147.
[23] I.R. Whittall, M.P. Cifuentes, M.G. Humphrey, B. Luther-Davies, M. Samoc, S. Houbrechts, A. Persoons, G.A. Heath, D. Bogsanyi, Organometallics 16 (1997) 2631.
[24] A.M. McDonagh, M.P. Cifuentes, I.R. Whittall, M.G. Humphrey, M. Samoc, B. Luther-Davies, D.C.R. Hockless, J. Organomet. Chem. 526 (1996) 99.
[25] A.M. McDonagh, I.R. Whittall, M.G. Humphrey, B.W. Skelton, A.H. White, J. Organomet. Chem. 519 (1996) 229.
[26] A.J. Hodge, S.L. Ingham, A.K. Kakkar, M.S. Khan, J. Lewis, N.J. Long, D.G. Parker, P.R. Raithby, J. Organomet. Chem. 488 (1995) 205.
[27] R.H. Naulty, M.P. Cifuentes, M.G. Humphrey, S. Houbrechts, C. Boutton, A. Persoons, G.A. Heath, D.C.R. Hockless, B. Luther-Davies, M. Samoc, J. Chem. Soc. Dalton Trans. (1997) 4167.
[28] B.D. Yeomans, D.G. Humphrey, G.A. Heath, J. Chem. Soc. Dalton Trans. (1997) 4153.
[29] B.D. Yeomans, PhD Thesis, Australian National University, 1995.
[30] B.J. Coe, C.J. Jones, J.A. McCleverty, D. Bloor, G. Cross, J. Organomet. Chem. 464 (1994) 225.
[31] M. Lequan, R.M. Lequan, K.C. Ching, J. Mater. Chem. 1 (1991) 997.
[32] D.R. Kanis, M.A. Ratner, T.J. Marks, J. Am. Chem. Soc. 112 (1990) 8203.
[33] D.R. Kanis, M.A. Ratner, T.J. Marks, J. Am. Chem. Soc. 114 (1992) 10338.
[34] C.W. Dirk, H.E. Katz, M.L. Schilling, L.A. King, Chem. Mater. 2 (1990) 700.
[35] A.K. Jen, P. Rao, K.Y. Wong, K.J. Drost, J. Chem. Soc. Chem. Commun. (1993) 90.
[36] L. Cheng, W. Tam, S.R. Marder, A.E. Steigman, G. Rikken, C.W. Spangler, J. Phys. Chem. 95 (1991) 10643.
[37] L. Cheng, W. Tam, S.H. Stevenson, G.R. Meredith, G. Rikken, S.R. Marder, J. Phys. Chem. 95 (1991) 10631.
[38] T. Sakamoto, M. Shiraiwa, Y. Kondo, H. Yamanaka, Synthesis (1983) 312.
[39] B. Chaudret, G. Commenges, R. Poilblanc, J. Chem. Soc. Dalton Trans. (1984) 1635.
[40] J. Chatt, R.G. Hayter, J. Chem. Soc. (1961) 896.
[41] teXsan, Single Crystal Structure Analysis Software, Version 1.7-3, 1995, Molecular Structure Corporation, The Woodlands, Texas, USA.
[42] M. Stähelin, D.M. Burland, J.E. Rice, Chem. Phys. Lett. 191 (1992) 245.
[43] E. Hendrickx, C. Dehu, K. Clays, J.L. Brédas, A. Persoons, in: G.A. Lindsay, K.D. Singer (Eds.), Polymers for Second-Order Nonlinear Optics, American Chemical Society, Washington DC, 1995, p. 82.
[44] K. Clays, A. Persoons, Rev. Sci. Instrum. 63 (1992) 3285.
[45] S. Houbrechts, K. Clays, A. Persoons, Z. Pikramenou, J.-M. Lehn, Chem. Phys. Lett. 258 (1996) 485.